arXiv:cond-mat/0009041v2 [cond-mat.str-el] 9 Mar 2001

Commensurate-Incommensurate transition in the melting process of the orbital ordering in $Pr_{0.5}Ca_{0.5}MnO_3$: neutron diffraction study

R. Kajimoto
Department of Physics, Faculty of Science, Ochanomizu University, Bunkyo-ku, Tokyo 112-8610, Japan

H. Yoshizawa
Neutron Scattering Laboratory, Institute for Solid State Physics, University of Tokyo, Tokai, Ibaraki, 319-1106, Japan

Y. Tomioka
Joint Research Center for Atom Technology (JRCAT), Tsukuba, Ibaraki 305-8562, Japan

Y. Tokura
Joint Research Center for Atom Technology (JRCAT), Tsukuba, Ibaraki 305-8562, Japan
Department of Applied Physics, University of Tokyo, Bunkyo-ku, Tokyo 113-8656, Japan

(February 1, 2008)

The melting process of the orbital order in $Pr_{0.5}Ca_{0.5}MnO_3$ single crystal has been studied in detail as a function of temperature by neutron diffraction. It is demonstrated that a commensurate-incommensurate (C-IC) transition of the orbital ordering takes place in a bulk sample, being consistent with the electron diffraction studies. The lattice structure and the transport properties go through drastic changes in the IC orbital ordering phase below the charge/orbital ordering temperature $T_{\mathrm{CO/OO}}$, indicating that the anomalies are intimately related to the partial disordering of the orbital order, unlike the consensus that it is related to the charge disordering process. For the same T range, partial disorder of the orbital ordering turns on the ferromagnetic spin fluctuations which were observed in a previous neutron scattering study.

64.70.Rh, 71.27.+a, 71.30.+h, 71.45.Lr

Charge ordering is an ubiquitous phenomenon in transition metal oxides. For example, a so-called "CE-type" charge ordering plays an essential role in the Colossal Magnetoresistance (CMR) phenomenon which can be observed in hole-doped perovskite manganites, such as $R_{1-x}A_x\mathrm{MnO}_3$, where R denotes trivalent rare-earth ions while A denotes divalent alkaline-earth ions.[1,2] In the CE-type charge-ordered state which appears near $x \sim 1/2$, Mn^{3+} and Mn^{4+} ions form a checkerboard pattern with a $1:1$ ratio. As pointed out in pioneering works on $La_{0.5}Ca_{0.5}MnO_3$ by Wollan and Koehler[3] and Goodenough,[4] this charge-ordered state is accompanied with the ordering of the e_g orbitals on Mn^{3+} sites as well as the CE-type antiferromagnetic (AFM) spin ordering,[5,6] thereby offering an ideal platform to study an interplay among charge, orbital and spin degrees of freedom.

Reflecting such multiple degrees of freedom, the CE-type charge/orbital/spin ordering shows a complicated ordering/melting process. According to very recent x-ray scattering studies on $Pr_{1-x}Ca_xMnO_3$ with $x \sim 1/2$, the simultaneous charge/orbital long-range ordering is formed at $T_{\mathrm{CO/OO}}$. Well above $T > T_{\mathrm{CO/OO}}$, however, the charge/orbital short-range correlation is developed, but the correlation length of the short-range charge ordering ξ_{CO} is always longer than that of the orbital ordering ξ_{OO}, indicating that the charge ordering is a driving force for the CE-type charge/orbital ordering.[7,8] As for the spin correlations, the CE-type AFM long-range spin order is established at T_{N} which is far below $T_{\mathrm{CO/OO}}$, and the AFM spin fluctuations in the charge/orbital-ordered phase is rapidly taken over by the ferromagnetic fluctuations in the T region for $T_{\mathrm{N}} \lesssim T \lesssim T_{\mathrm{CO/OO}}$.[9]

One of the interesting but not well-elucidated aspects of the CE-type charge/orbital ordering transition is the incommensurability of the orbital ordering. When the ideal CE-type charge/orbital order is formed, zigzag arrangement of the ordered $d(3x^2-r^2)$ and $d(3y^2-r^2)$ orbitals of Mn^{3+} ions in the ab plane and associated lattice distortions will double the unit cell along the b axis in the orthorhombic ($Pbnm$) lattice, and produce commensurate superlattice reflections at $\boldsymbol{q}_{\mathrm{OO}} = (0,\, 1/2,\, 0)$.[5,10] In contrast to these expectations, based on electron diffraction studies, it has been repeatedly reported that the CE-type charge/orbital ordering in $La_{0.5}Ca_{0.5}MnO_3$ and $R_{1-x}\mathrm{Ca}_x\mathrm{MnO}_3$ with $x \sim 1/2$ (R: rare-earth ions) is incommensurate,[10–16] and an elaborate charge/orbital ordering (or melting) process was suggested. In particular, it was argued that the onset of the commensurate orbital ordering is decoupled from the onset of the charge ordering, and the orbital ordering can be incommensurate immediately below $T_{\mathrm{CO/OO}}$. In fact, the incommensurability[17] ϵ in $Pr_{0.5}Ca_{0.5}MnO_3$ observed by electron diffraction becomes finite above the AFM spin ordering temperature T_{N}, and ϵ grows with increasing T, reaching as large as $0.11 \sim 0.12$ near $T_{\mathrm{CO/OO}}$.[12–16] It should be noted that such a large value of ϵ has been observed mainly in electron diffraction studies or an x-ray study with $\mathrm{La_{0.5}Ca_{0.5}MnO_3}$ powder sample.

By contrast, very recent x-ray scattering studies on single crystal samples of $\mathrm{Pr_{1-x}Ca_xMnO_3}$ argued that the orbital ordering wave vectors remain strictly commensurate throughout the ordered phase at any temperature, being in striking disagreement with the electron diffraction studies.[8,18] Incidentally, there is no explicit statement on the incommmensurability from neutron diffraction studies to our knowledge, seemingly giving an impression that the charge/orbital ordering may be commensurate. A lack of consensus on this issue over three diffraction techniques may give rise to a question whether the incommensurate orbital ordering is an intrinsic bulk property.

To unravel this issue, neutron diffraction would be a key experimental technique because of high transmissibility of neutrons which allows to observe bulk properties of the specimen. Moreover, the neutron diffraction has an advantage that it is sensitive to the displacements of oxygen ions which are introduced by the orbital ordering. In what follows, we shall report a detailed neutron diffraction study of the melting process of the orbital ordering in a single crystal sample of $\mathrm{Pr_{0.5}Ca_{0.5}MnO_3}$. We shall demonstrate that the orbital ordering is indeed *incommensurate* for certain temperature range below $T_{\mathrm{CO/OO}}$, and argue that the anomalies are intimately related to the disordering process of the orbital order, unlike the conventional picture that it is related to the collapse of the charge ordering.

$\mathrm{Pr_{0.5}Ca_{0.5}MnO_3}$ is orthorhombic, but is very close to cubic.[5,16] Throughout this paper, we employ the *Pbnm* setting for convenience of easier comparison with preceding works. Thereby, the lattice constants are related to the simple cubic lattice parameter a_c as $a \sim b \sim c/\sqrt{2} \sim \sqrt{2}a_c \sim 5.4$ Å. In the *Pbnm* setting, the superlattice reflections due to the orbital ordering appear at $(h,\ k/2,\ l)$ with $k =$ odd integer at low temperatures. The CE-type AFM Bragg reflections by the $\mathrm{Mn^{3+}}$ moments appear at $(h/2,\ k,\ l)$ with $k =$ integer and $h, l =$ odd integer, while those by the $\mathrm{Mn^{4+}}$ moments appear at $(h/2,\ k/2,\ l)$ with $h,\ k,\ l =$ odd integer.

The single crystal sample was melt-grown by the floating zone method as described elsewhere.[1] The quality of the sample was checked by x-ray powder diffraction measurements and by inductively coupled plasma mass spectroscopy (ICP). Neutron diffraction experiments were performed using a triple axis spectrometer GPTAS installed at the JRR-3M reactor in JAERI, Tokai, Japan. The incident neutron momentum is $k_{\mathrm{i}} = 2.66$ Å^{-1} with a pyrolytic graphite (PG) filter employed before the sample to suppress higher-order contaminations. Most of the measurements were carried out with a double axis configuration with $20'$-$20'$-$20'$ collimators, while for measurements at high temperature ($T \geq 250$ K) the collimation was relaxed to $20'$-$40'$-$20'$ or $20'$-$40'$-$40'$ to improve the visibility of weak superlattice peaks. The sample was mounted in an Al can filled with He gas, and was attached to the cold head of a closed-cycle helium gas refrigerator. The temperature was controlled within an accuracy of 0.2 K. All the measurements were carried out on the $(h,\ k,\ 0)$ scattering plane except for the T dependence of the AFM Bragg reflection $(0.5,\ 0.5,\ 1)$.

In order to confirm the presence of the superlattice peaks due to lattice modulations induced by the orbital ordering, we surveyed the $(h,\ k,\ 0)$ scattering plane at 100 K. The superlattice peaks were observed at the $(h,\ k \pm 1/2,\ 0)$ positions with $h, k =$ integer. The peak intensity shows a strong Q dependence due to the structure factor, and for an accessible Q range of the present experiments, the strong peaks were observed along the $(2,\ k,\ 0)$ line, and the profiles around $(2,\ -0.5,\ 0)$ scanned along k at selected T's are shown in Fig. 1. Since the charge/orbital ordering transition is weakly first order with hysteresis (See Fig. 2(d)), all the measurements in the present study were carried out with elevating T. The magnetic and charge/orbital ordering transition temperatures for the present sample are $T_{\mathrm{N}} \sim 180$ K and $T_{\mathrm{CO/OO}} \sim 240$ K, respectively (See Fig. 2(a)). In the left column of Fig. 1, one can see a well-defined peak centered at $k = -0.5$ up to $T \sim 220$ K, indicating that the orbital order is commensurate. Even for the moderate momentum resolution of neutron diffraction, the peak has a finite width, indicating that the orbital ordering is not a true long range order. From the width of profiles, the correlation length ξ for the orbital ordering is roughly estimated to be an order of ~ 100

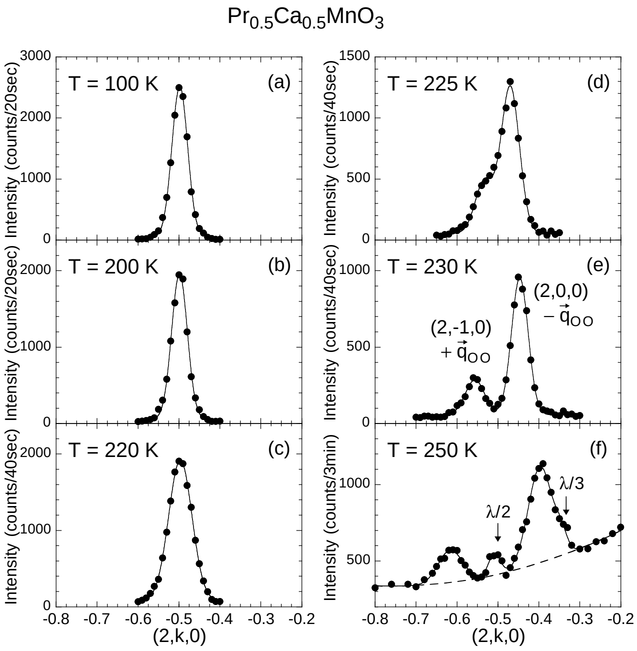

FIG. 1. Temperature dependence of the orbital ordering superlattice peak observed along the [010] direction at selected T's. Note that $T_{\mathrm{N}} \sim 180$ K and $T_{\mathrm{CO/OO}} \sim 240$ K, respectively. The peak at $k = -1/2$ and the shoulder at $k = -1/3$ in (f) are contaminations due to the higher-order reflections.

Å at 100 K, being consistent with the x-ray scattering study ($\xi = 160 \pm 10$ Å).[8] The finite correlation length of the orbital ordering also limits the correlation length of the accompanied CE-type AFM spin ordering, as was demonstrated in recent neutron diffraction studies.[9,10,16]

At $T = 220$ K, the width is slightly wider than those at lower T's, but it recovers the low T value for 225 K $\lesssim T \leq T_{\mathrm{CO/OO}}$, and the profile splits into two peaks at the incommensurate positions $(2, -0.5 \pm \epsilon, 0)$.[17] Upon elevating T above $T_{\mathrm{CO/OO}} \sim 240$ K, the width increases rapidly, while the intensity decreases drastically. As shown in Fig. 1(f), the intensity of the superlattice peaks at $T = 250$ K is now weaker than a tail of the Huang scattering centered at $Q = (2, 0, 0)$ which was observed in a recent x-ray measurement.[18,19] As labeled in Fig. 1(e), the weak peak at left and the stronger peak at right are assigned to $(2, -1, 0) + \boldsymbol{q}_{\mathrm{OO}}$ and $(2, 0, 0) - \boldsymbol{q}_{\mathrm{OO}}$ with $|\boldsymbol{q}_{\mathrm{OO}}| = 0.445$, respectively. From the scattering configuration, it is straightforward to see that the superlattice intensity results from the transverse component of the lattice distortions induced by the orbital ordering because of the $|\boldsymbol{Q} \cdot \boldsymbol{\eta}|^2$ term in the cross section, where $\boldsymbol{\eta}$ represents a displacement vector of constituent ions. Furthermore, an asymmetry of superlattice intensities reflects the difference of the structure factor of generic fundamental nuclear Bragg reflections, weak $(2, -1, 0)$ and intense $(2, 0, 0)$ reflections. It should be noted that similar two peak profiles with asymmetric intensity in $\mathrm{Pr_{0.5}Ca_{0.5}MnO_3}$ were clearly observed in electron diffraction studies,[12,15] but not observed in recent x-ray studies.[8,18]

Now that the incommesurability of the orbital ordering has been confirmed by the present neutron diffraction study, we shall examine the melting process of the orbital ordering in further detail. In Fig. 2(a) are plotted the T dependences of the order parameter of the CE-type AFM spin ordering for the $\mathrm{Mn^{4+}}$ moments observed at $\boldsymbol{Q} = (0.5, 0.5, 1)$ and that of the orbital ordering observed around $\boldsymbol{Q} = (2, -0.5, 0)$ with elevating T. The CE-type AFM spin ordering disappears at $T_{\mathrm{N}} \sim 180$ K. The T dependence of the orbital order parameter in Fig. 2(a) exhibits a clear change at $T_{\mathrm{C-IC}} \sim 215$ K. The intensity decreases gradually up to $T_{\mathrm{C-IC}}$, then drops steeply towards $T_{\mathrm{CO/OO}} \sim 240$ K. Interestingly, this changeover of the T dependence of the intensity corresponds to the commensurate-to-incommensurate transition of the orbital ordering vector $\boldsymbol{q}_{\mathrm{OO}} = (0, \delta, 0)$, as is shown in Fig. 2(b). Up to $T_{\mathrm{C-IC}} \sim 215$ K, the peak position is commensurate with $\delta = 0.5$, then δ gradually decreases towards $\delta \sim 1/3$. Namely, the orbital ordering in $\mathrm{Pr_{0.5}Ca_{0.5}MnO_3}$ is incommensurate for $T_{\mathrm{C-IC}} \lesssim T \lesssim T_{\mathrm{CO/OO}}$. The T dependence of the width of the superlattice peak is also shown in the same panel. The width shows a subtle increase around $T_{\mathrm{C-IC}}$ which is also evident in the profile shown in Fig. 1(c), but recovers and maintains the low T value up to $T_{\mathrm{CO/OO}}$. The T region of the incommensurate orbital ordering corresponds exactly to the precipitous change of the lattice constants as evidenced by the T dependence of the scattering vector for the (2, 0, 0) nuclear Bragg reflection (Fig. 2(c)), and a steep decrease of the resistivity (Fig. 2(d)).

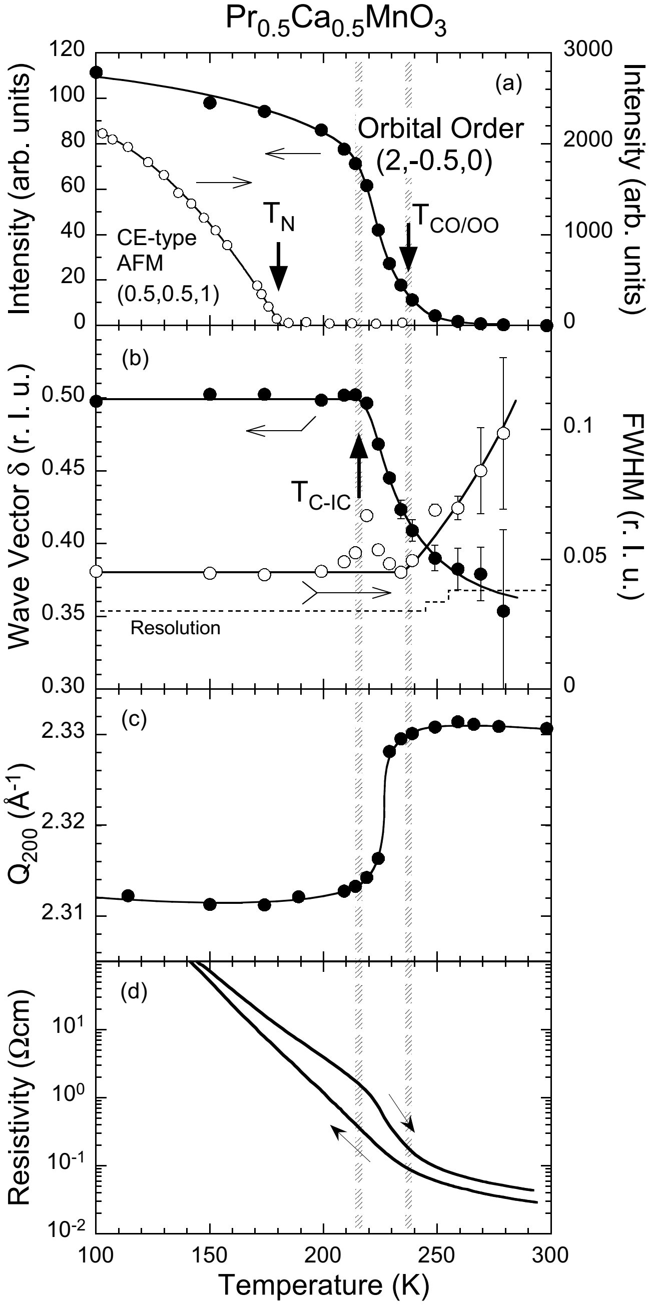

FIG. 2. T dependences of (a): Integrated intensities for (2, −0.5, 0) orbital order peak (closed symbols) and (1/2, 1/2, 1) AFM peak (open symbols). (b): Orbital order wave vector $\boldsymbol{q}_{\mathrm{OO}} = (0, \delta, 0)$ (closed symbols) and width (FWHM) of (2, −0.5, 0) orbital order peak (open symbols). (c): Scattering vector of the (2, 0, 0) fundamental reflection. (d): Resistivity. In (b), the instrumental resolution is indicated as a dotted line. All data except the resistivity were measured with heating.

From the data presented in Fig. 2, the following intriguing picture emerges for the melting process of the orbital ordering in $\mathrm{Pr}_{0.5}\mathrm{Ca}_{0.5}\mathrm{MnO}_3$. The melting process consists of three stages. First of all, the C-IC transition of the orbital ordering is not correlated to the CE-type spin ordering at $T_{\mathrm{N}} \sim 180$ K, and begins at $T_{\mathrm{C-IC}} \sim 215$ K. In a very early stage of the C-IC transition, the superlattice is still almost commensurate, but its width increases (Fig. 1(c)), indicating that the commensurate and nearly-commensurate orbital orders are mixed in the system. This stage may be attributed to the situation in which occasional discommensurations are introduced to the system. According to high resolution lattice images, it is suggested that unpaired Mn^{3+} stripes cause discommensurations.[13,14] In the second stage of the transition, the superlattice peak splits into two incommensurate peaks. At the same time, the lattice constants show precipitous changes, and the incommensurability varies quickly, although the width recovers the low T value. The decrease of the superlattice intensity above $T_{\mathrm{C-IC}}$ indicates that the number of the orbital-disordered Mn^{3+} ions rapidly increases in the system. Concomitantly, the local melting of the orbital ordering triggers the rearrangement of the local Jahn-Teller lattice distortions, and causes the change of lattice constants (Fig. 2(c)). This rearrangement process also triggers the steep decrease of the resistivity (Fig. 2(d)). In the third stage above $T_{\mathrm{CO/OO}}$, the charge ordering and quasi-long-range orbital ordering is destroyed, and their correlation lengths rapidly increase. By $T_{\mathrm{CO/OO}}$, the local Jahn-Teller lattice distortions are sufficiently relaxed, then a rapid change of the lattice constants disappears above $T_{\mathrm{CO/OO}}$ (Fig. 2(c)).

It should be noted that in a study of the CE-type ordering the charge and orbital orderings are often considered to take place at the same temperature, because the CE-type charge and orbital orders are strongly coupled and their transition temperatures are very close. By careful examination of the melting process of the orbital ordering, however, we succeeded in establishing that the anomalies in the structural, transport and magnetic properties take place in the IC orbital ordering state below the charge ordering temperature $T \sim T_{\mathrm{CO/OO}}$. The present results indicate that the importance of distinguishing the gradual melting process of orbital ordering from the collapse of charge ordering in order to understand the nature of the physical properties in the CMR manganites.

It is also noteworthy that the partial disordering of the orbital order is consistent with the onset of ferromagnetic spin fluctuations previously reported.[9] Kajimoto *et al.* reported that the ferromagnetic spin fluctuations are developed for $T_{\mathrm{N}} \lesssim T \lesssim T_{\mathrm{CO/OO}}$. In the melting process of the C-IC orbital ordering, a partially disordered orbital order disturbs static AFM exchange paths, and gives rise to ferromagnetic spin fluctuations. In this sense, the C-IC orbital disordering process is intimately related to the ferromagnetic spin fluctuations.

In summary, we have studied the melting process of the orbital ordering in $\mathrm{Pr}_{0.5}\mathrm{Ca}_{0.5}\mathrm{MnO}_3$ single crystal as a function of T by neutron diffraction measurements. We successfully demonstrated that an incommensurate orbital ordering certainly exists in a bulk sample. The quasi long-range orbital ordering persists well above the C-IC transition temperature $T_{\mathrm{C-IC}}$. The incommensurate melting of the orbital order induce the rearrangement of the lattice structure and the steep decrease of the resistivity due to partial disordering of the orbital order, and also induce ferromagnetic spin fluctuations which was reported in the previous neutron scattering study. This fact indicates that the drastic anomalies in charge/orbital ordered manganites are caused by the change of the orbital order rather than the charge order.

This work was supported by a Grand-In-Aid for Scientific Research from the Ministry of Education, Science, Sports and Culture, Japan and by the New Energy and Industrial Technology Development Organization (NEDO) of Japan.

---

[1] Y. Tomioka, A. Asamitsu, Y. Moritomo, and Y. Tokura, J. Phys. Soc. Jpn. **64**, 3626 (1995); Y. Tomioka, A. Asamitsu, H. Kuwahara, Y. Moritomo, and Y. Tokura, Phys. Rev. B **53**, R1689 (1996).

[2] H. Kuwahara, Y. Tomioka, A. Asamitsu, Y. Moritomo, and Y. Tokura, Science **270**, 961 (1995).

[3] E.O. Wollan and W.C. Koehler, Phys. Rev. **100**, 545 (1955).

[4] J.B. Goodenough, Phys. Rev. **100**, 555 (1955).

[5] Z. Jirák, S. Krupička, Z. Šimša, M. Dlouhá, and S. Vratislav, J. Magn. Magn. Mater. **53**, 153 (1985).

[6] H. Yoshizawa, H. Kawano, Y. Tomioka, Y. Tokura, Phys. Rev. B **52**, R13145 (1995); J. Phys. Soc. Jpn. **65**, 1043 (1996).

[7] M. v. Zimmermann, J.P. Hill, Doon Gibbs, M. Blume, D. Casa, B. Keimer, Y. Murakami, Y. Tomioka, and Y. Tokura, Phys. Rev. Lett. **83**, 4872 (1999).

[8] M. v. Zimmermann, C.S. Nelson, J.P. Hill, Doon. Gibbs, M. Blume, D. Casa, B. Keimer, Y. Murakami, C.-C. Kao, C. Venkataraman, T. Gog, Y. Tomioka, and Y. Tokura, cond-mat/0007231 (unpublished).

[9] R. Kajimoto, T. Kakeshita, Y. Oohara, H. Yoshizawa, Y. Tomioka, Y. Tokura, Phys. Rev. B **58**, R11837 (1998).

[10] P.G. Radaelli, D.E. Cox, M. Marezio, S-W. Cheong, Phys. Rev. B **55**, 3015 (1997).

[11] C.H. Chen and S-W. Cheong, Phys. Rev. Lett. **76**, 4042 (1996).

[12] A. Barnabé, M. Hervieu, C. Martin. A. Maignan, and B. Raveau, J. Mater. Chem. **8**, 1405 (1998); J. Appl. Phys. **84**, 5506 (1998).

[13] S. Mori, C.H. Chen, and S-W. Cheong, Phys. Rev. Lett. **81**, 3972 (1998).

[14] C.H. Chen, S. Mori, and S-W. Cheong, Phys. Rev. Lett.

83, 4792 (1999).

[15] S. Mori, T. Katsufuji, N. Yamamoto, C.H. Chen, and S-W. Cheong, Phys. Rev. B **59**, 13573 (1999).

[16] Z. Jirák, F. Damay, M. Hervieu, C. Martin, B. Raveau, G. André, and F. Bourée, Phys. Rev. B **61**, 1181 (2000).

[17] The incommensurability ϵ is defined as $\boldsymbol{q}_{\rm OO} = (0,\, 1/2 - \epsilon,\, 0)$ from the observed position of the superlattice peaks.

[18] S. Shimomura, T. Tonegawa, K. Tajima, N. Wakabayashi, N. Ikeda, T. Shobu, Y. Noda, Y. Tomioka, and Y. Tokura, Phys. Rev.B **62**, 3875 (2000).

[19] The scan profile consists of two components: one is the superlattice peak of the orbital ordering, and the other is the Huang scattering. Since they have completely different physical origins, they should be strictly distinguished.